Multi-Colour and Tunable-Colour Pyroelectric Detectors

Norbert Neumann, Martin Ebermann, Kerstin Schreiber, Matthias Heinze
InfraTec GmbH, Dresden, Germany

ABSTRACT

Multi-colour and tunable colour pyroelectric detectors are compared in respect of gas analysis. The key elements of the detectors are a beam splitter and a Fabry-perot filter respectively. The beam splitter are micromachined plates with pyramids or V-grooves with a pitch of 100…150 µm to ensure a homogeneous distribution of the radiation flux. Narrow bandpass filters are arranged at a filter cage forming a four sided frustum of pyramid. The angle of 30° for the micro pyramids and the filter cage guarantees that the radiation hits the filter perpendicular. The tunable filter is a MEMS based fabry-perot filter. It is based on an approach using relatively thick reflector carriers, one of them being fixed and the other suspended by springs with compensating elements. In order to achieve the tuning of the resonator cavity, an electrostatic actuation using a parallel plate design has been chosen. Short and long cavity filters were designed for the spectral ranges of 5.0…3.7 µm and 4.3…3.0 µm respectively. Spectral flat, blackened pyroelectric chips are arranged behind the filters in both the multi-colour and tunable-colour detectors. Beam splitting results in a time parallel split-up and filtering of the incident radiation flux, whereas in the tunable-colour detector, the filtering is a time serial process.

Keywords: Infrared gas analysis, Beam splitter, Fabry-Perot filter, Infrared filter, Bragg reflector, Anti-reflection coating, bulk micromachining,

1. INTRODUCTION

Infrared gas analysers are based on the absorption of infrared radiation. These systems determine the concentration of a specific gas by measuring the amount of radiation absorbed at specific wavelengths, corresponding to electronic transitions in the molecules being detected. In figure 1, the discrete absorption bands of carbon monoxide, carbon dioxide, propane, methane, and nitrous oxide are shown in the range from 3...5 µm as an example.

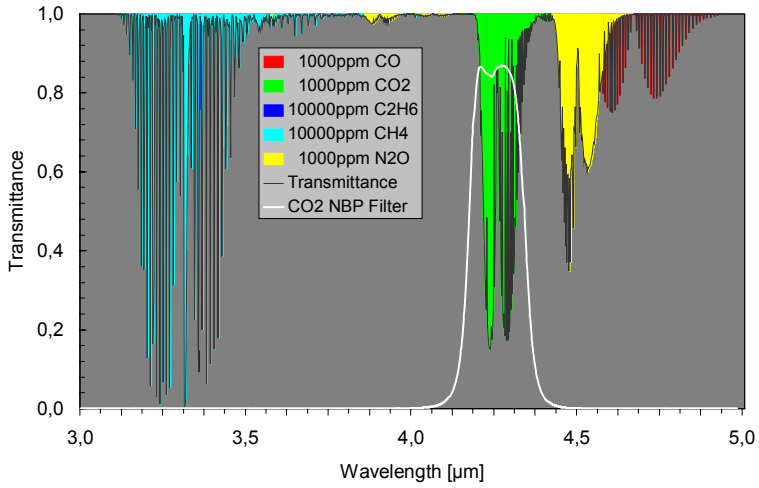

Fig. 1. Transmission of different gases and of a CO_2 Near Bandpass filter in the 3…5 µm band (T = 273 K, p = 1013hPa, l = 5 cm) /1/

Methods using filters for analysing a broadband emitter spectrum, play a major role in industrial and medical gas analysis. Often such filter photometers are ranked among non-dispersive methods. This is not completely correct, as the filters themselves rely on the interference principle /2/.

The analyser, schematically shown in fig. 2 includes a sample chamber for holding a sample gas, a radiation emitter for directing a beam through the chamber and a detector for indicating the amount of radiation absorbed. Pyroelectric detectors are widely used as a result of their advantages, like room temperature operation, robustness, flat spectral response and low costs. The narrow band infrared filters are selected in accordance to the substances to be analysed. The bandwidth of the filter is much broader than a single absorption line and could be several percent of the centre wavelength. For CO_2 measurements, for instance a filter with a centre wavelength of 4.26 µm and a bandwidth of

90…180 nm is commonly used (see figure 1). Often an additionally reference channel is used to cancel intensity shifts of the IR emitter.

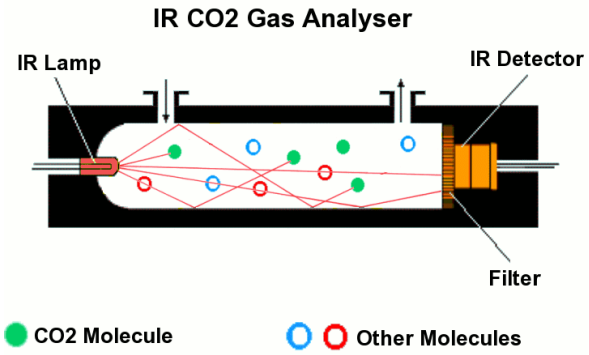

Fig. 2. Schematic of an infrared filter gas analyser

Different methods are developed to analyse mixtures with different substances simultaneously. One is the known filter wheel method. A plurality of filters, each of which transmit radiation at an absorption band of a gas component to be detected, are alternately positioned in the radiation path to produce a time-multiplexed signal having the concentration information for all gases.

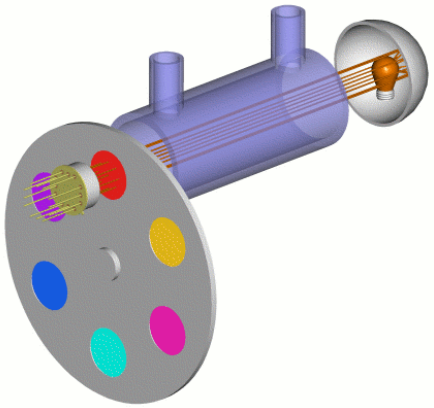

Fig. 3. Principal of a filter wheel photometer

Detectors with separate spectral channels are developed to overcome the drawbacks of size, power consumption and mechanical sensitivity of the filter wheel method. A simple approach is the combination of several detection units in a common package to form a multi-colour detector. The narrowband filters are arranged in one plane. Therefore, the diameter of the gas cell is increased. An additional problem appears from radiation unbalance caused by inhomogeneous changes of the reflectance of the cell wall or from changes of the position of the radiation emitter for instance of the filament of a incandescent lamp. InfraTec provides two solutions for this problem with a parallel and a serial spectral filter mode:

1. the multi-colour detector with integrated beam splitter and
2. the tunable-colour detector with integrated Fabry-Perot filter

2. MULTI-COLOR DETECTOR

The principle of the multi-colour detector with integrated beam splitter is shown in figure 4. The IR radiation entering through the aperture stop is divided by a beam splitter in four parts. Each of the partial beam is going through an IR filter and hits a pyroelectric detector chip. The beam splitters are made of gold plated microstructures with a pitch of 100 µm or 150 µm respectively, to achieve a homogeneous distribution of the radiance. The filters are arranged under a certain angle to obtain a normal incidence of the radiation. This assembling avoids the drifting of the filter transmission curves to shorter wavelengths and the influence of the opposite filter

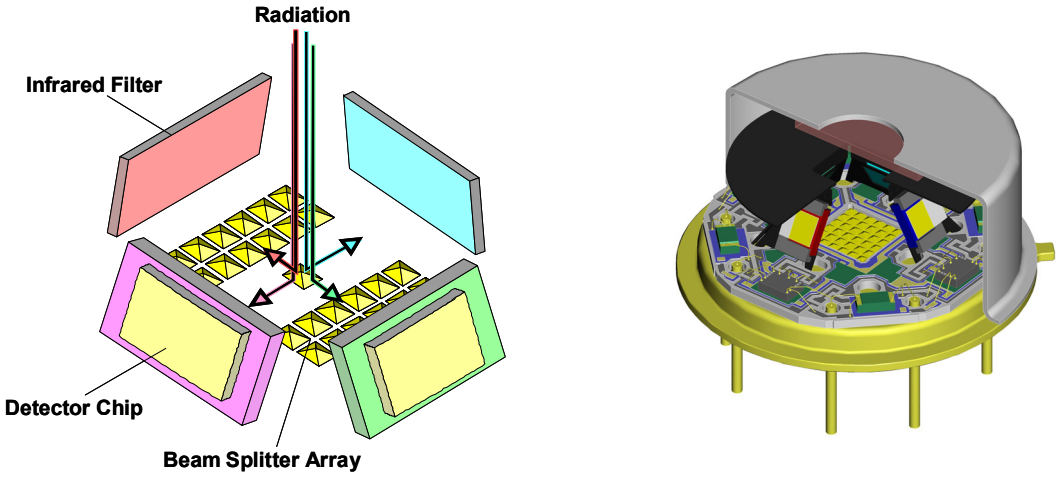

Fig. 4. Principal and schematic drawing of a multi-colour detector with integrated beam splitter

As the beam splitter detector compared to other multi-channel detectors has only one aperture stop, it is possible to use a gas cell with a smaller diameter reducing the gas volume. A smaller gas volume reduces the size of the sensor module and accelerates the gas-exchange. In addition to four-channel beam splitter detectors using four-sided micro pyramids, InfraTec also applies two-channel detectors based on micro V-grooves. In fig.5 SEM images of two- and four-channel beam splitters are shown. Whereas the pitch of the V-groves and the pyramids is varying between 100 µm and 150 µm, the tilt angle amounts 30°. During manufacturing it is essential to realize extremely sharp edges to minimize the reflection deviating from 30°.

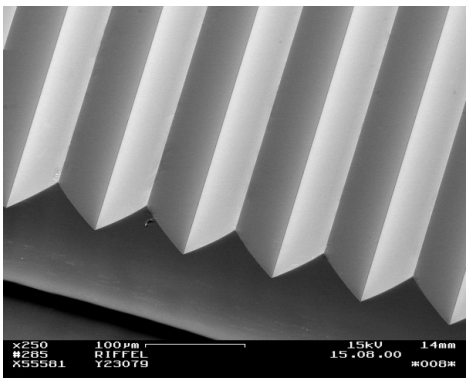

Fig. 5a. SEM image of a two channel beam splitter

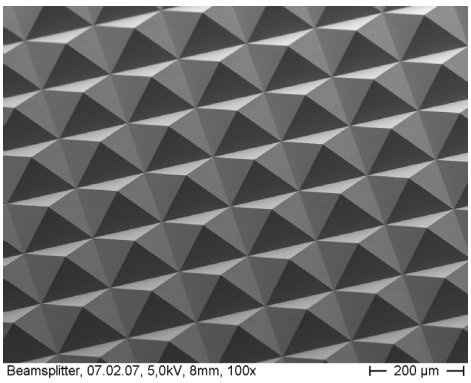

Fig. 5b. SEM image o four channel beam splitter

In fig 6 the spatial sensitivity distribution of one single channel of a beam splitter detector with different types of beam splitter designs and arrangements of beam splitters is demonstrated. The measurement was conducted by scanning the aperture of 2.5 mm by a laser spot with a diameter of 100 µm. The left picture shows the responsivity distribution using a 10x10 pyramid structure and a 30° filter cage, whereof in the centre a 4x4 pyramid structure and a 30° filter cage was used. On the right a single four-sided pyramid and a 15° filter cage was used. Using a beam splitter with remarkably larger and in a 4x4 grid arranged micro pyramids the homogeneity is unsatisfactory, however the application of a beam splitter with 10x10 micro pyramids leads to a sufficient composition of the single beams, resulting in a good homogeneity of the responsivity. The right hand figure shows that a single pyramid and a filter cage, which additionally uses the reflected fraction of the opposite filter, is completely inapplicable. This beam guiding originates “ghost” figures.

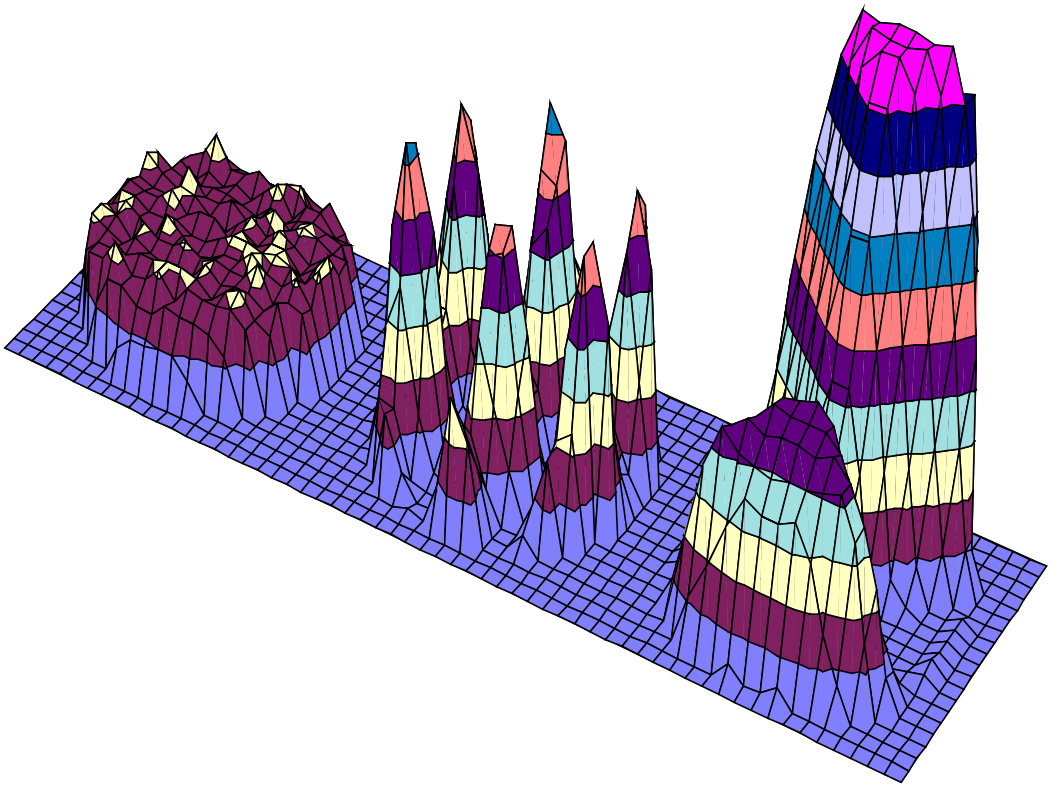

Fig. 6 Spatial distribution of the relative responsivity of a single channel with different types of beam splitter designs and arrangements of beam splitters (left: 10x10 micro pyramid beam splitter / 30°-filter cage, centre: 4x4 micro pyramid beam splitter / 30°-filter cage, right: single pyramid beam splitter / 15° filter cage)

3. TUNABLE-COLOR DETECTOR

The design principle of the tunable-colour detector is shown in figure 7. The tunable filter is a MEMS based fabry-perot filter. It is based on an approach using relatively thick reflector carriers, one of them being fixed and the other suspended by springs which allow vertical movement. A set-up of coated and etched wafer is bonded directly or by an intermediate SU-8 layer. This yields in medium fabrication complexity. In order to achieve the tuning of the resonator cavity, an electrostatic actuation using a parallel plate design has been chosen.

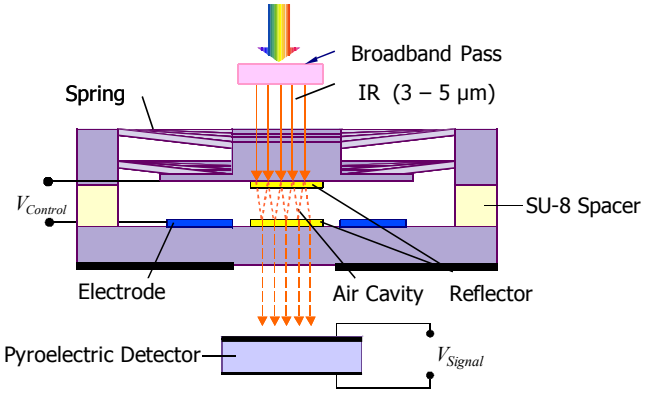

Fig. 7. Design principle of the detector with tunable filter

The tunable filter is arranged on top of a pyroelectric detector with a flat spectral response, shown in figure 8. Both, the tunable filter and the detector, are packaged in a TO-8 housing with a broad bandpass filter. The broad bandpass filter transmits only in the tuning range of the filter and blocks higher interference orders and long wave radiation.

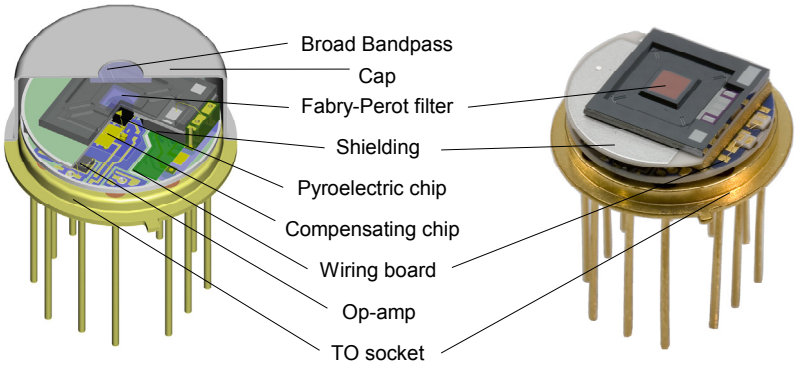

Fig. 8. Schematic drawing (left) and picture of a sample (right) of a tunable pyroelectric detector with integrated filter

A classical Fabry-Perot interferometer is the key element of the MEMS based tunable IR filter, which is built up of an optical resonator consisting of two coplanar reflectors with a separation distance d and a material with a refraction index n in between them. By varying the separation distance d, the filter can be spectrally tuned. In figure 9 the set-up principle and the transmission as function of the wavelength λ is presented.

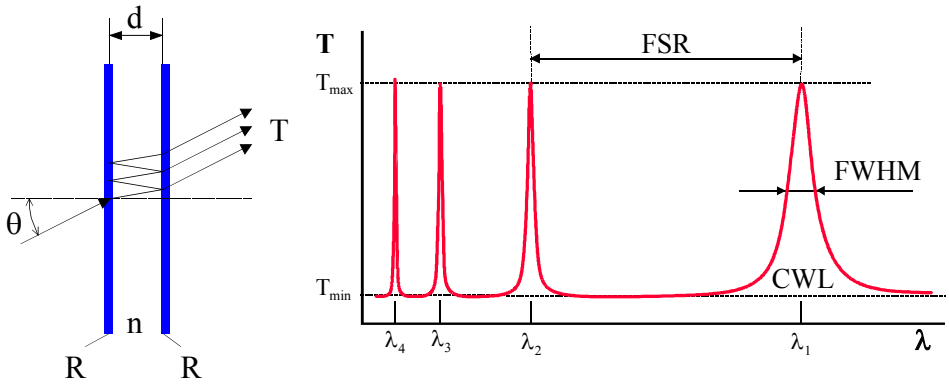

Fig. 9. Schematic arrangement principle and transmission spectra of the Fabry-Perot interferometer (FSR: Free Spectral Range; FWHM: Full Width at Half Measure; CWL: Centre Wavelength)

The tunability of the filter between 5 µm and 3 µm requires an order number *m = 1* and a physical adjustment of the resonator cavity with a distance d of about 2500 nm to 1500 nm. Bandwidths of 100…50 nm require a finesse (the ratio of FSR to FWHM) between 40…80 or a reflectance of the coplanar reflectors of 92…96 % respectively.

Distributed Bragg reflectors are commonly used to generate a broadband reflector /3/. Bragg reflectors are built up by alternating quarter wave optical thickness (QWOT) layers with low (L) and high (H) refractive index, forming a (LH) periods. In order to generate a broad high reflective zone from 3…5 µm even with a low period number, thin films with as high as possible refractive index ratio n_H/n_L have to be applied. This is shown in fig. 10, in which the reflectance of a Bragg reflector with different layer periods at the reference wavelength (3.5 µm) is plotted against the ratio of the refractive indices, n_H/n_L. Additionally, the bandwidth (at 90 % reflectance) of a reflector with period number of 2 is calculated against the ratio of the refractive indices, n_H/n_L.

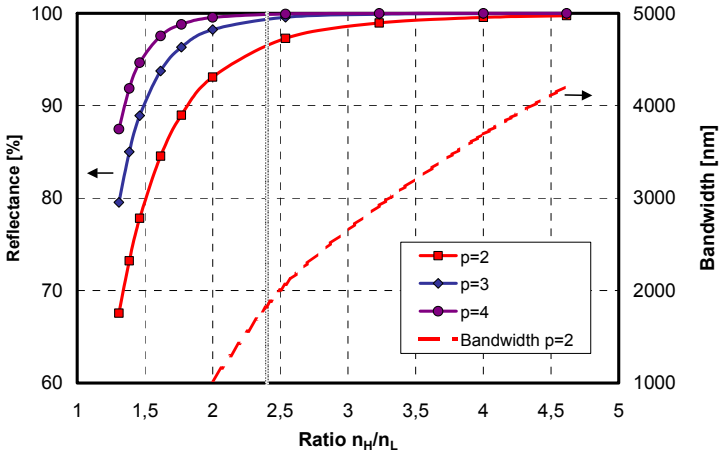

Fig. 10. Reflectance of Bragg reflectors at the reference wavelength of 3.5 µm and bandwidth vs. ratio of the refractive indices for different layer periods

Silicon dioxide with a refractive index of 1.38 at 4 µm is used as low refractive index material and polycrystalline silicon with a refractive index of 3.33 at 4 µm is used as high refractive index material for the reflectors. The layers are deposited by CVD processes. Because of the high ratio of refractive indexes n_H/n_L of 2.41 a wide high-reflective zone from 3…5 µm with a high average and maximum reflectance of about 95% and of 96% respectively was obtained already with a $|LH|^2$ layer stack /4/.

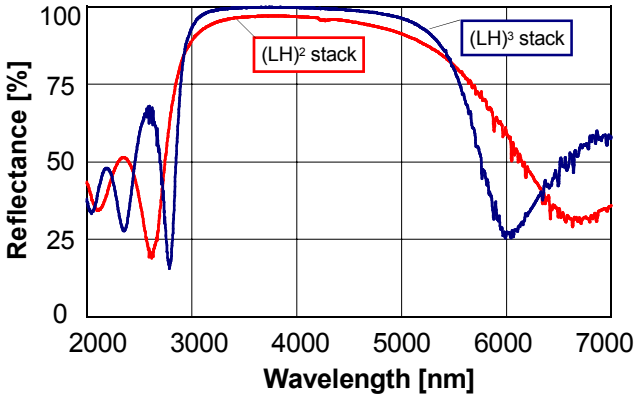

Fig. 11. Spectral reflectance of silicon substrates with layer stacks

Increasing the period number to 3 the average and maximum reflectance increases to 98 % and 99 % respectively and squares the high reflection zone (see fig. 11). Otherwise the roughness of the stack increases, resulting in a remarkable worse performance /5/. Hence a double-stack $|LH|^2$ was chosen as Bragg reflector and the spectral range of 3…5 µm was divided in two sub-ranges with each 1300 nm from 3.0...4.3 µm und 3.7...5.0 µm.

The backsides of the wafer were anti-reflection coated to reduce reflection losses and ripples in the high reflective band caused by multiple reflections in the silicon substrate. Single QWOT layers show a reflectance minimum only at the reference wavelength, which is presented fig. 12a Alternatively a multi-layer design increases the transmittance in a broader wavelength range. This design uses only a QWOT silicon dioxide layer for the first layer and very thin films of silicon dioxide and polycrystalline silicon fulfilling the condition $nd << \lambda$ to match a medium refractive index /6/.

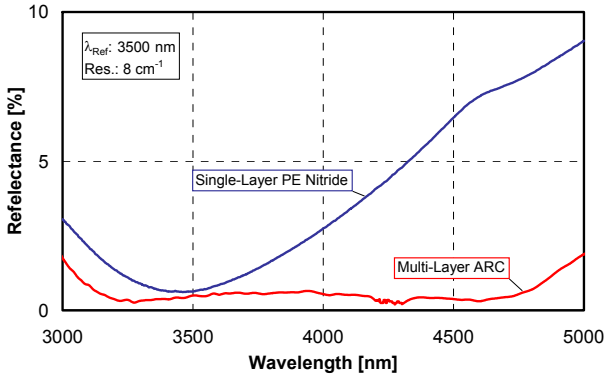

Fig. 12a. Reflectance of single and multi-layer layer anti-reflection coating

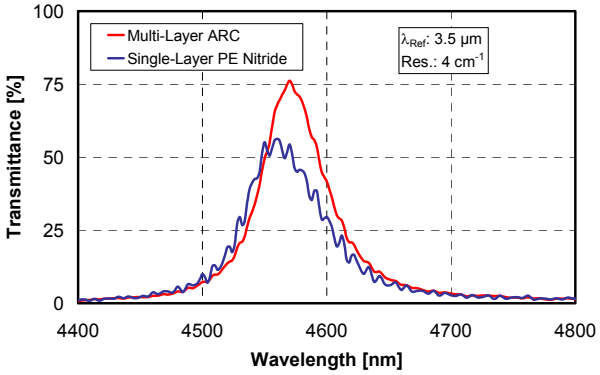

Fig.12b Transmittance fringes of FP filters with Si_3N_4 single layer and a multi-layer ARC

The reflectance of the refined triple-layer ARC has an average of 0.6% in the hole spectral range of 3…5 µm and a minimum of 0.3%. In fig. 12b, it is also shown that the multi-layer ARC reduces the ripple amplitude and increases the transmittance much better then a single layer ARC out of range of the reference wavelength.

The FP filter is fabricated by bulk micromachining technology to achieve optimum interference conditions. High resistivity silicon wafers with a thickness of 300 µm are used as carriers for both the fixed and the movable reflector. The fixed reflector is located in the centre surrounded by the driving electrodes. The movable reflector is suspended by diagonally arranged springs located in the corners of the outer frame. Various types of movable reflectors and spring configurations have been fabricated to determine the optimum solution with respect to maximum tuning range, low gravity influence on centre wavelength and filter bandwidth, low deviation of reflector parallelism by mechanical stress and low fabrication complexity /7/. The parallel spring design results in a nearly ideal movement in vertical direction. But this is only the case, if the assembling of the planes succeeds tension and warping free. Tensions in lengthwise direction cannot be compensated by the springs. They lead to a deformation of the spring in vertical direction shown in fig. 13.

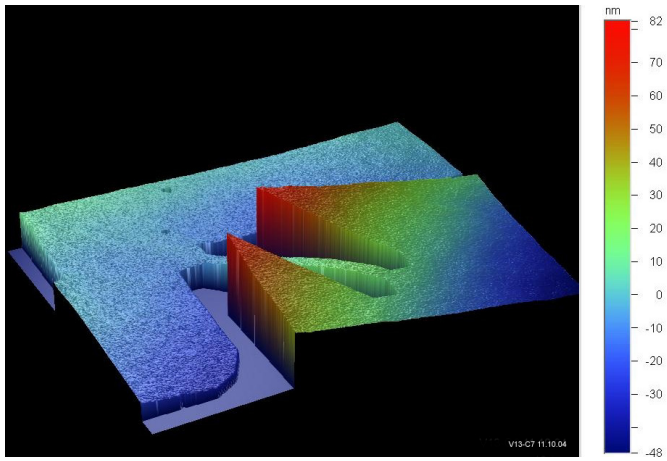

Fig 13. Flatness measurement results on a filter with parallel spring design (measured by WYKO NT1100)

Alternatively stress compensation elements can be integrated into the springs, which is shown in figures 14a and 14b. The T-form facilitates the reception of tensions in lengthwise direction, as the small T side can be bended crosswise. Advantages of this modification are the simple and proven technology, a large freedom of the design parameters and the high precision of the fabricated springs. The dry etching makes it possible to manufacture smaller dimensions of the spring and also smaller trenches. Thus the spring needs less space even with complicated embodiment and more area can be used for the electrostatic force generation. Combined with a wet etching process for the adjustment of the spring thickness, very precise spring mass systems can be produced.

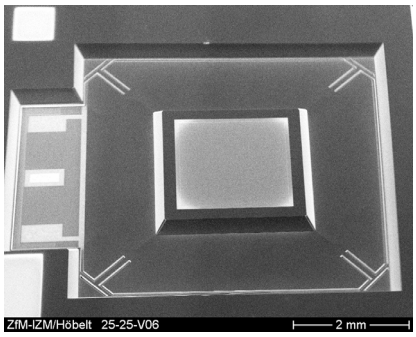

Fig. 14a. SEM image of the single wafer movable reflector carrier fabricated by dry etching

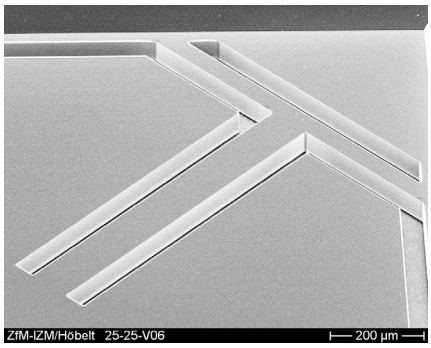

Fig. 14b. SEM image of the dry etched springs with a stress compensating element

The results of the transmittance measurements of the short and long cavity filters presented in figures 15 and 16 confirm the optical design to achieve a high transmittance and a low bandwidth. The typical bandwidths *FWHM* of the long cavity and short cavity filters are 100±20 nm and 80±20 nm respectively. The voltage dependence of the filter's *CWL* features the typical square root function of an electrostatic actuator. The decreasing transmittance during tuning is a result of the moveable reflectors tilting, which is induced from spring stiffness and electrode area inhomogeneities. The spring design with compensation elements results in maximum driving voltages 27 V to provide a tuning range of about 1300 nm.

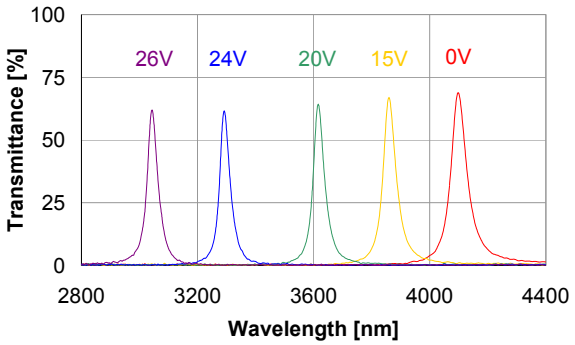

Fig. 15a. Spectral transmittance of a short cavity FP filter

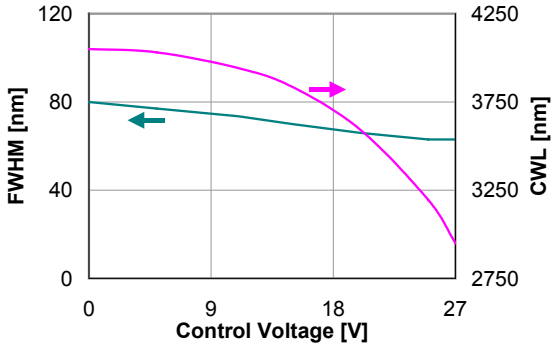

Fig. 15b Bandwidth and center wavelength of a short cavity FP filter

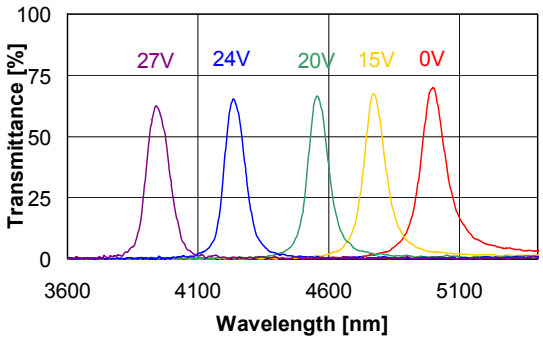

Fig. 16a. Spectral transmittance of a long cavity FP filter with low stiffness compensating springs

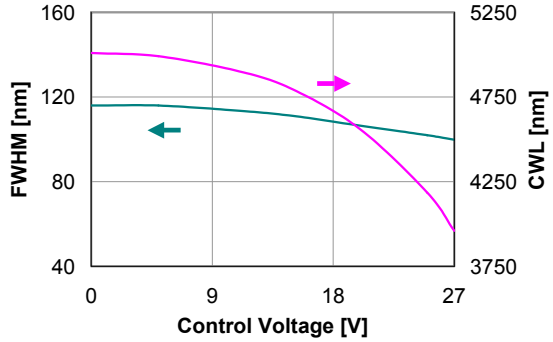

Fig. 16b. Bandwidth and center wavelength of a long cavity FP filter

4. COMPARISON OF MULTI-COLOR AND TUNABLE COLOR DETECTORS

Both detectors can be used in current mode as well as in voltage mode. The respective circuitries are shown in fig. 17. The specific detectivity D* of pyroelectric detectors is equal in both modes for identical basic conditions. Even so, the current mode has some advantages, with the result, that this is the preferred mode in tunable colour detectors. Because of the considerably lower electrical time constant the responsivity above the thermal time constant is some orders of magnitude higher. The amplitude characteristic is very flat up to the electric corner frequency, which can be in the range of 10….1000 Hz /8/.

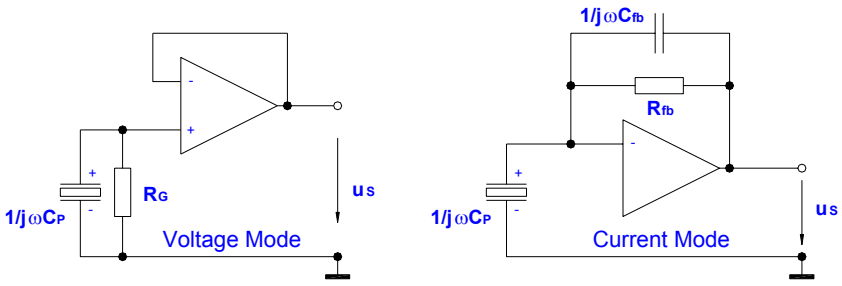

Fig. 17: Schematic circuit of voltage and current mode of pyroelectric detectors

Multi-colour detectors separate the beam entering through the aperture stop in two or four parts, which halves or quarters the total radiation flux. However, the beam splitting and spectral filtering are carried out at the same time. For the tunable-colour detector the spectral filtering is a sequential process, where the whole radiation flux which is entering the aperture stop is available. The near band pass filters of the multi-colour detectors are also based on the design principle of a Fabry-Perot filter and use dielectric QWOT layers for reflectors and resonator-cavity. In contrast to the tunable

Fabry-Perot filter the NBP's can have multiple coupled cavities. Thus a more rectangular transmission curve is reached, which results in a higher effective transmission of the filters and a better adjustment with the gas absorption band..

The multi-colour detector should be preferably used for the analysis of gas mixtures with few, known gases. Typical examples for a successful application are anaesthetic gas monitors and the pulmonary function testing. Tunable-colour detectors allow a more flexible operation of the analyser enabling the detection of adjoining or overlapping absorption bands. So far the measurement of single gases like ethanol and carbon dioxide as well as gas mixtures of methane, propane and anaesthetic gases have been tested. In table 1 multi- and tunable-colour detectors are summarized.

Table 1: Comparison of multi and tunable colour detectors

Specification	**Multi colour detector**	**Tunable colour detector**
Principal	Beam splitter	Tunable Fabry-perot Filter
Filtering	Parallel	Serial
Radiation flux per channel	25or 50 %	100 %
filter	Single and multi-cavity	Single tunable air cavity
Spectral range	(3…25) µm	(4.3…3.0) /(5.0…3.7) µm
Current mode	Yes	Yes
Voltage mode	Yes	Yes
Thermal Compensation	No	Yes

REFERENCES

1. MolExplorer 3.6, Copyright 2006 PASTECH GmbH
2. J. Staab, *Industrielle Gasanalyse*, Oldenbourg, München und Wien, 1994.
3. H.A. Macleod, *Thin-Film optical filters*, IoP, Bristol and Philadelphia, 2001.
4. S. Kurth, K. Hiller, N. Neumann, M. Heinze, W. Dötzel, T. Geßner, "A tunable Fabry-Perot-Interferometer for 3–5 µm wavelength with bulk micromachined reflector carrier", Proc. SPIE Vol. 4983, 215-226 (2003).
5. N. Neumann, K. Hiller and S. Kurth, „Micromachined Mid-Infrared Tunable Fabry-Perot Filter", Proc. 13th Int. Conf. on Solid-State Sensors, Actuators and Microsystems, 1010-1013 (2005) Seoul, Korea, June 5-9, (2005).
6. W.H. Stockwell, "Coating design using very thin high- and low-index layers", *Appl. Optics* 24(4), 457-460 (1985).
7. N. Neumann, M. Ebermann, K. Hiller , S. Kurth, „Tunable infrared detector with integrated micromachined Fabry-Perot filter", Proc. SPIE Vol. 6466, 646606 1-12; (2007)
8. N. Neumann, H.-J. Stegbauer, H. Sänze, M. Gürtner, F. Schneider, „Application of fast response dual-colour pyroelectric detectors with integrated op amp in a low power NDIR gas monitor", Proc. 8th Int. Conf. for Infrared Sensors and systems, IRS2, 183-188 (2004), Nuremberg, Germany, 25-27 May, 2004.